Vision Res. Vol. 33, No. 7, pp. 993–999, 1993
Printed in Great Britain.

0042-6989/93 $6.00 + 0.00

Lateral Interactions Between Spatial Channels: Suppression and Facilitation Revealed by Lateral Masking Experiments

URI POLAT,* DOV SAGI*

Received 20 January 1992; in revised form 31 August 1992

We measured contrast detection thresholds for a foveal Gabor signal flanked by two high contrast Gabor signals. The spatially localized target and masks enabled investigation of space dependent lateral interactions between foveal and neighboring spatial channels. Our data show a suppressive region extending to a radius of two wavelengths, in which the presence of the masking signals have the effect of increasing target threshold. Beyond this range a much larger facilitatory region (up to a distance of ten wavelengths) is indicated, in which contrast thresholds were found to decrease by up to a factor of two. The interactions between the foveal target and the flanking Gabor signals are spatial-frequency and orientation specific in both regions, but less specific in the suppression region.

Lateral masking Lateral inhibition Spatial filters Segmentation

1. INTRODUCTION

The existence of channels in the human visual system, which are selectively sensitive to different ranges of spatial frequencies (Campbell & Robson, 1968; Graham & Nachmias, 1971; Graham & Robson, 1987; Sachs, Nachmias & Robson, 1971; Sagi & Hochstein, 1983; Tolhurst & Barfield, 1978; Watson, 1982) and orientations (Kulikowski, Abadi & King-Smith, 1973) is indicated by increasing evidence. The outputs of these channels are detected independently when the channels receive different inputs, which requires that activity in one channel does not affect the activity of channels responding to other ranges of spatial frequencies, orientations or spatial locations. Apparently the neural channels underlying this stimulus selectivity are not completely independent and receive inhibitory inputs from channels coding for neighboring spatial frequencies or orientations and disinhibitory inputs from channels beyond this inhibitory region (De Valois, 1977; Greenlee & Magnussen, 1988; Tolhurst & Barfield, 1978). These interactions are assumed to be restricted to channels having spatially overlapping receptive fields.

Considering the local nature of spatial filters one can expect to find some interactions between neighboring channels. Such a network of interconnections may underline human ability to analyze image properties higher than those obtained from local luminance variations. Experimental evidence for local spatial interactions comes from studies involving subjective contrast estimations (Cannon & Fullenkamp, 1991a; Chubb, Sperling & Solomon, 1989; Sagi & Hochstein, 1985). These studies indicate the existence of local inhibitory connections between spatial filters having similar orientation and spatial frequency selectivity. It was suggested that these interactions reduce human sensitivity to uniform textural fields and enhances our ability to detect texture borders (Sagi, 1990). These latter studies, involving detection of textural singularities (orientation pop-out, e.g. detecting a target element within a dense texture of orthogonal elements) indicate an antagonistic connectivity field around each channel, having an excitatory radius of three times filter wavelength and an inhibitory surround extending up to a distance of nine wavelengths. While lending support for the existence of some type of lateral inhibitory network in early stages of visual processing, the above mentioned studies employ visual tasks of somewhat higher complexity than those used in standard low level visual experiments. Both search tasks (or textural singularities detection) and subjective contrast judgment tasks may address a level of processing higher than the one uncovered by threshold detection tasks.

This study was performed to elucidate the spatial interactions between channels sensitive to different spatial locations. We used standard contrast detection tasks, under conditions of lateral masking. Three Gabor signals: a Gabor target located in the foveal region, between two masking Gabor signals positioned with identical eccentricity were utilized. Changes in detection threshold induced by the flanking masking Gabor as a function of their eccentricity were measured. One important difference between our study and earlier ones on

*Department of Neurobiology, Brain Research, The Weizmann Institute of Science, Rehovot 76100, Israel.

lateral masking (Bouma, 1970; Flom, Weymouth & Kahneman, 1963b; Flom, Heath & Takahashi, 1963a) is the choice of stimuli, in our case band limited Gabor signals while in the earlier studies alphanumeric characters were used. The psychophysical task differed also in a significant way: earlier studies employed letter recognition or gap detection (in a Landolt C) tasks, while we used a two-alternative forced-choice contrast detection paradigm. We believe that these differences are important in distinguishing between two major contributions to the masking effect. The first being from within filter integration processes (assumed to be linear) while the second is from between filter interactions (following some nonlinearity at the filter output). In particular, the use of localized band-pass stimuli provides us with a better control over the set of filters (or channels) activated by the stimulus, by minimizing the number of active units. Since filter size is assumed to be about two times its most sensitive wavelength (Watson, Barlow & Robson, 1983; Wilson, 1983), we expect to find interactions from within the filters integration processes within this range. The situation is somewhat more complicated when using low-pass stimuli as letters (Bouma, 1970), line elements (Kulikowski & King-Smith, 1973) or light spots (Westheimer, 1967), which are lowpass and broad band in the spatial frequency domain and thus, when considering lateral interferences, probe mainly within filter integration process by activating relatively large (lower frequency) filters that cover both the test and the mask. Indeed, earlier studies involving detection of a light spot on a background of a larger adapting field were interpreted in terms of retinal inhibition (Westheimer, 1967). Later studies involving detection of a fine line flanked by two masking lines were interpreted in terms of linear integration within spatial filters (Kulikowski & King-Smith, 1973). In a similar way, masking experiments using spatially overlapping narrow band gratings as mask and test probe within filter integration or integration between spatially overlapping filters of different peak frequencies, depending on the frequency difference between test and mask (Harvey & Doan, 1990; Daugman, 1984; De Valois, 1977). As a compromise between using overlapping gratings or nonoverlapping line elements, we used spatially displaced Gabor signals as test and mask (Gabor, 1946). Although giving up complete localization in both space and frequency domain, this configuration seems to be more suitable to explore interactions between spatially adjacent filters.

2. METHODS

Apparatus

Stimuli were displayed as gray-level modulation on an Hitachi HM-3619A color monitor, using an Adage 3000 raster display system. The video format was 56 Hz noninterlaced, with 512×512 pixels occupying a 9.6×9.6 deg area. The mean display luminance was 50 cd/m^2 in an otherwise dark environment. Stimulus generation was controlled by a Sun-3/140 workstation and the stimulus display by the Adage local processor. Gamma correction was applied using 10-bit lookup tables.

Stimuli

Stimuli consisted of three Gabor signals arranged vertically (see Fig. 1). The luminance distribution of one Gabor signal is determined by

$$L(x, y|x_0, y_0) = \cos\left(\frac{2\pi}{\lambda}((x - x_0)\cos\theta + (y - y_0)\sin\theta)\right)\exp\left(-\left(\frac{(x - x_0)^2 + (y - y_0)^2}{\sigma^2}\right)\right) \quad (1)$$

where x is along the horizontal axis, y the vertical axis, θ the orientation of the Gabor signal (in radians), λ the

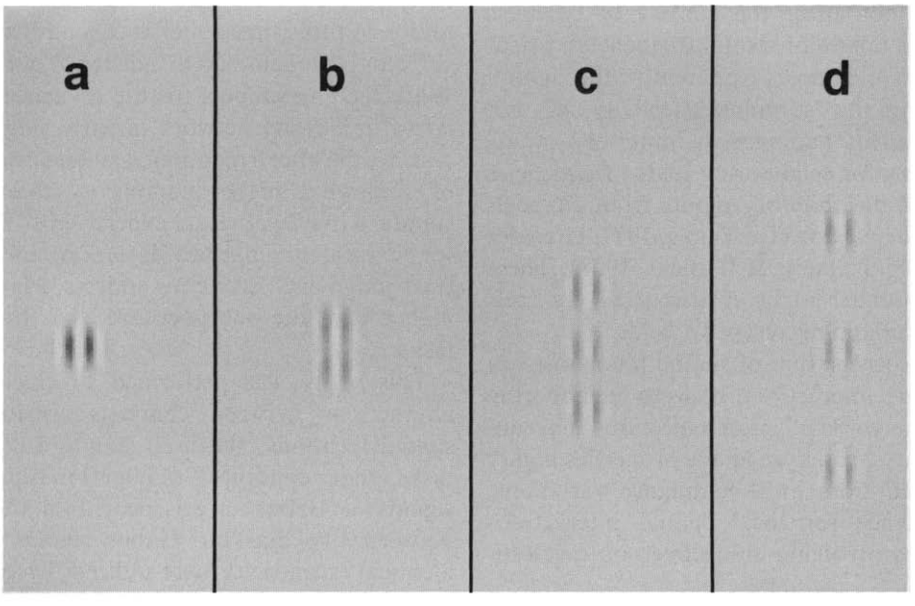

FIGURE 1. Stimuli configurations demonstrating some target to mask distances used in the present experiments. Distance (center to center) = 0λ (a), 1.5λ (b), 3λ (c) and 6λ (d). Here target contrast (central patch) is somewhat enhanced for demonstration purpose, see Methods for more details.

wavelength and σ the standard deviation of the Gaussian envelop. The summation of three Gabor signals shifted by Δx and Δy, as specified by equation (2), describes the stimuli used in these experiments.

$$L(x,y|x_0,y_0) = A_m L(x,y|x_0 - \Delta x, y_0 - \Delta y) + A_t L(x,y|x_0,y_0) + A_m L(x,y|x_0 + \Delta x, y_0 + \Delta y) + I \quad (2)$$

A_m and A_t are the mask and target amplitudes respectively and I is the average screen luminance. In all cases the masks were aligned along the vertical meridian ($\Delta x = 0$, Δy = variable) and x_0,y_0 coincided with the fixation point for all experiments described below. In most experiments we used vertical targets and masks so that varying only the vertical mask to target distance did not affect relative phase. The Gaussian envelope size (0.075 or 0.15 deg) was selected so to have at least one cycle within a range of $\pm\sigma$ from the Gaussian center. Target and mask wavelength were varied between 0.075 and 0.3 deg. In all experiments, unless otherwise defined, mask amplitude (A_m) was 30% of mean luminance ($0.3I$) for $\Delta y < 3\lambda$ and 40% otherwise. This choice was made as a compromise between two constrains; one limiting the maximum contrast at small separations ($2A_m + A_t < I$), while on the other hand we wanted high mask contrast for large separations where the masks were pushed into the periphery. Data from pilot experiments show that at a test to mask distance of 3λ the effects we measured are independent of mask contrast within a relatively large range (20–80%).

Experimental procedures

A two-alternative temporal forced-choice paradigm was used. Each block consisted of 50 trials, across which the signal amplitude and the distance between the Gabor signals were kept constant. Each trial consisted of two stimuli presented sequentially only one of which had a target. Before each trial, a small fixation cross was presented at the center of the screen. When ready, the observers pushed a key activating the trial sequence: a no stimulus interval (randomized within a range of 360 ± 270 msec a stimulus presentation for 90 msec, a no stimulus interval (randomized within a range of 846 ± 270 msec), and a second stimulus presentation for 90 msec. Screen luminance (I) was kept constant during the stimulus and no stimulus intervals. Each stimulus display included two peripheral high contrast crosses, marking the target stimulus interval presentation. The observers task was to determine which of the stimuli contain the target. Auditory feedback, by means of a keyboard bell, was given on observers' error immediately after response. Psychometric curves were obtained for each spatial separation, from which contrast thresholds were estimated by curve fitting with the Quick function. Each point on the psychometric curve was based on at least 16 blocks of trials (800 trials). In some experiments, requiring many threshold estimates (Figs 4–7), a staircase method (Tolhurst & Barfield, 1978) was used to determine the threshold, yielding practically the same results (where a comparison can be made). When using staircase method, each threshold was estimated 4–8 times. SEs, where presented, are averages across observers where each observer's SE was obtained from 4–8 threshold estimates.

Observers

Four naive observers and one of the authors (UP) with normal or corrected to normal vision in both eyes participated in these experiments. The stimuli were viewed binocularly from a distance of approx. 180 cm.

3. RESULTS

Contrast detection thresholds for the foveal Gabor signal were determined for different distances [Δy in equation (2)] between the flanking Gabor signals and the foveal target. In the first set of experiments the target and mask assumed vertical orientation and were situated on the vertical meridian. The changes in contrast threshold, relative to standard (no mask) condition is plotted in Fig. 2 as a function of target to mask distance (in units of target wavelength). The existence of two zones, positive and negative, where contrast detection thresholds are affected by flanking Gabor maskers was observed. In the positive region, within an eccentricity of 2λ, contrast detection thresholds increased reaching a maximal threshold elevation at a distance one wavelength between the flanking Gabor signals and the target. Outside this region detection thresholds are reduced, resulting in a negative region. The zone of negative threshold elevation is wider than the positive one, starting at $1.5–2\lambda$, reaching a minimum at 3λ and progressively returning to the standard threshold by 12λ. This range is much larger than the signal size ($\sigma = \lambda$), thus the enhancement effect cannot be attributed to

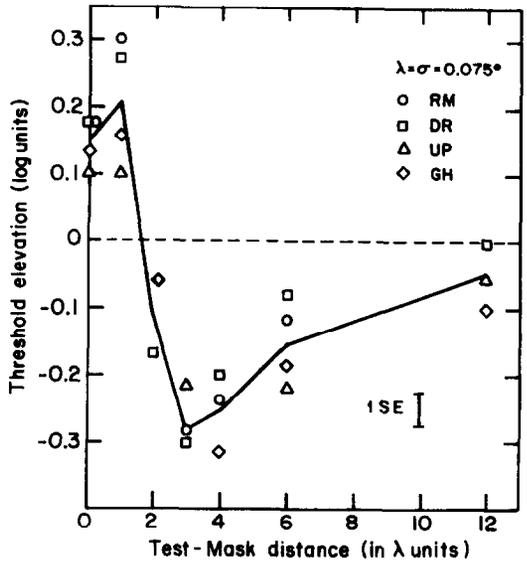

FIGURE 2. Dependence of target threshold on target to mask distance. Threshold elevation is computed relative to that of an isolated target. Data is presented for vertical target and masks ($\theta_t = \theta_m = 0$ deg, $\lambda_t = \sigma_t = \lambda_m = \sigma_m = 0.075$ deg) arranged along the vertical meridian ($\Delta x = 0$, Δy = distance). The detection threshold amplitude of the isolated target (A_t) was $0.14I$ for observer RM, $0.15I$ for DR, $0.17I$ for UP and $0.13I$ for GH.

signal overlap between test and mask (the area fraction under the two masks tails that fall within a range of $\pm\sigma$ from the test center is 0.045 for $\Delta y = 3\lambda$, 0.003 for $\Delta y = 4\lambda$ and practically zero for a distance of 6λ where enhancement is still significant). Additional control experiments using test and masks of opposite sign yielded practically the same results in the enhancement region, supporting the suggestion that enhancement effect is not due to linear integration.

In order to determine whether the above range of interactions depends on signal wavelength or on signal size, we repeated the measurements using Gabor signals of different wavelengths and thus different λ/σ values. Threshold data were obtained for target and masking Gabor signals having wavelengths of 0.075, 0.15, 0.225 and 0.3 deg and for different spatial separations. σ was 0.075 deg for the shortest wavelength and 0.15 deg for the others. Threshold elevation curves as a function of target to mask distance are depicted in Fig. 3 for the different spatial frequencies used. The threshold curves for all frequencies approximately overlap when plotted as a function of distance in units of signal wavelength. Although the high frequency curves seem to be shifted somewhat to the right, this shift is much smaller than would be expected from a constant interaction range (the shift is by a factor of 1.5 while a constant range would predict a factor of 4). The medium frequency curves, of 0.15 and 0.225 deg wavelength (dashed lines), are similarly shaped with the minima and maxima points close to those obtained with 0.075 and 0.3 deg. Thus, we can conclude that the relevant parameter is λ and not the signal size or some absolute spatial distance.

The specificity of the induced contrast threshold changes was examined for the orientations and spatial frequencies of the maskers, while keeping the target

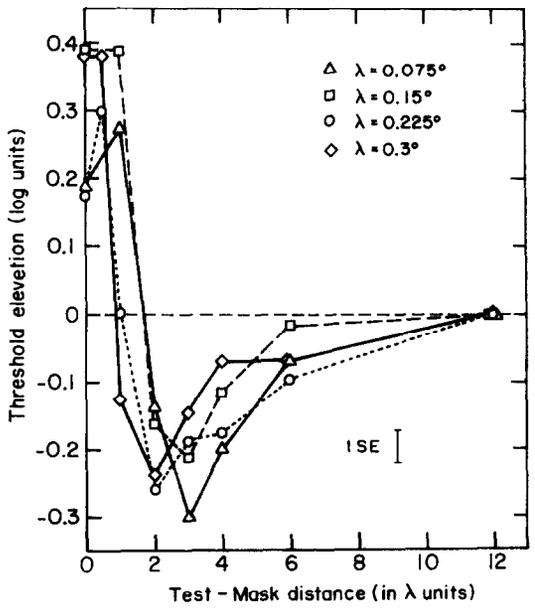

FIGURE 3. As for Fig. 2 but for target and mask wavelengths ($\lambda_t = \lambda_m$) of 0.075, 0.15, 0.225 and 0.3 deg. The detection threshold amplitude of the isolated target (A_t) was 0.15I for $\lambda_t = \sigma_t = 0.075$ deg, 0.05I for $\lambda_t = 0.15$ deg, $\sigma_t = 0.15$ deg and 0.04I for $\lambda_t = 0.225$ and 0.3 deg, $\sigma_t = 0.15$ deg (observer DR, $\sigma_m = \sigma_t$).

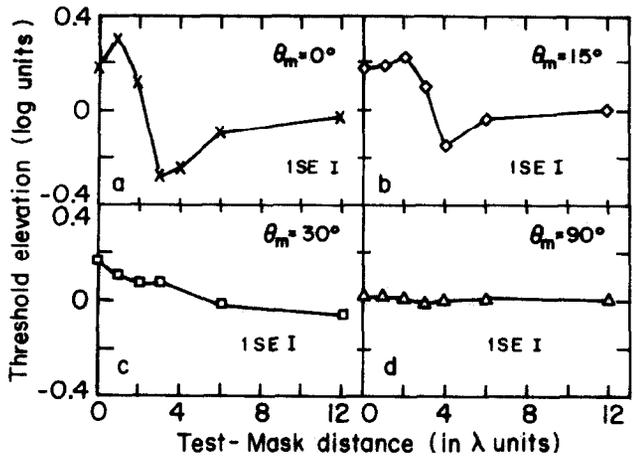

FIGURE 4. As in Fig. 2 but for different mask orientations (θ_m): 0 deg (a), 15 deg (b), 30 deg (c) or 90 deg (d) from the vertical. (Observer RM, $\lambda_t = \lambda_m = 0.075$ deg, $\theta_t = 0$ deg, $\sigma_t = \sigma_m = 0.15$ deg.) The detection threshold amplitude of the isolated target (A_t) was 0.05I.

constant. Figure 4 depicts threshold curves for a vertical (0 deg) Gabor signal, each curve for a different mask orientation. As can be seen from Fig. 4, the masking effect disappears when target and mask differ by 90 deg, but is still apparent at 15 deg difference. Also note that the negative lobe of the threshold curves seems to be somewhat more orientation selective than the positive lobe. This phenomenon can be better appreciated when examining Fig. 5. Here we present separately the orientation dependence of the minima and maxima points of the threshold curves. Maximal enhancement (in the negative zone) is decreased by a factor of two at 15 deg orientation difference, and asymptotes toward zero when the masking Gabor signals were presented at an orientation of 30 deg. On the other hand, a significant masking effect is still detectable in the positive zone for masks having an orientation of 45 deg.

The dependence of threshold elevation on target and mask spatial-frequency difference was studied and the

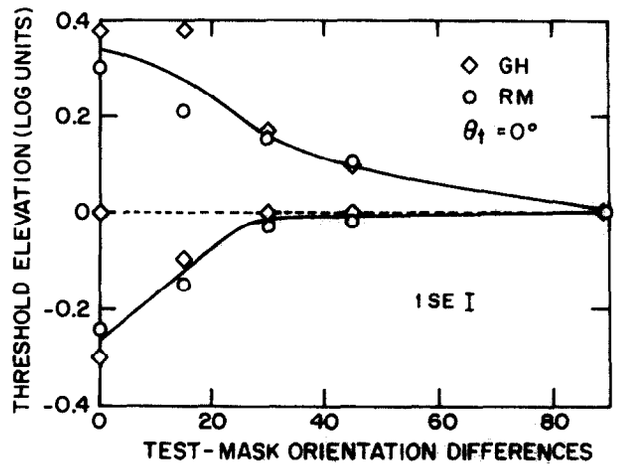

FIGURE 5. Maximal suppression and maximal enhancement as a function of mask–test orientation differences. The threshold elevation values were taken from curves as in Fig. 4, where maximal and minimal points were visually estimated. Curves were obtained by averaging the two observers' data points (RM and GH, where RM's data is presented in Fig. 4).

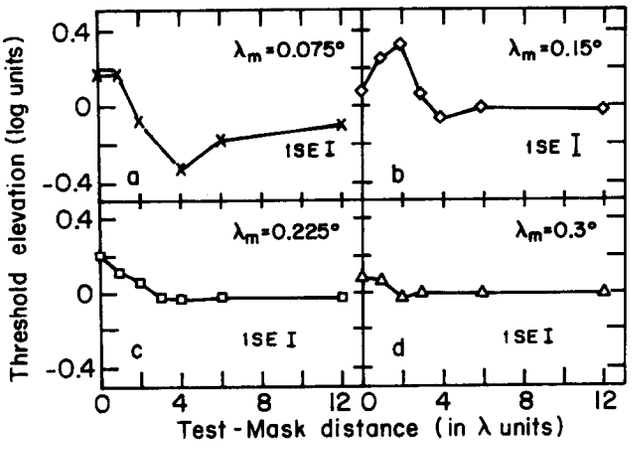

FIGURE 6. As in Fig. 2 but for different mask wavelengths (λ_m): 0.075 deg (a), 0.15 deg (b), 0.225 deg (c) and 0.3 deg (d). Observer GH, $\lambda_t = 0.075$ deg, $\theta_t = \theta_m = 0$ deg, $\sigma_t = \sigma_m = 0.15$ deg. The detection threshold amplitude of the isolated target (A_t) was 0.05*I*.

data is presented in Figs 6 and 7. Threshold elevation values corresponding to maximal enhancement and maximal suppression are depicted in Fig. 7 as a function of the ratio between mask to target wavelengths (λ_m/λ_t). The curves (averaged across observers) show narrower spatial frequency selectivity for the enhancement effect. The data depicted in Fig. 7 was obtained using two different target wavelengths, 0.075 deg where $\lambda_m \geq \lambda_t$ and 0.225 deg for $\lambda_m \leq \lambda_t$. As a result of this choice we obtained different threshold elevation estimates in the case of $\lambda_m = \lambda_t$; for $\lambda_t = 0.075$ deg and $\lambda_t = 0.225$ deg. Note also that the standard errors of the suppression estimate are larger than those of the enhancement estimates. This difference probably reflects instability due to practice (Sagi & Polat, 1992) and can be seen here also in the data of observer GH which was tested again after one year of practice (solid diamond in Fig. 7).

4. DISCUSSION

In this study we examined the effect of lateral masking on target detection. We observed both an increase and decrease of target thresholds in the presence of spatially adjacent high contrast signals. Threshold elevation was observed for target to mask distance smaller than twice the target wavelength. A decrease in threshold was observed when the distance ranged between two wavelengths and ten wavelengths. This pattern of results was obtained for cases where the maskers were displaced from the target in a direction defined by the orientation of target signal (Fig. 2). Increasing target and mask size (σ) by a factor of two did not affect the interaction range. In most cases the decrease in threshold was of equal or higher magnitude when compared with the increase in threshold, and more sensitive to differences between target and mask spectra. In all cases no significant effects were found when target and mask orientations differed by more than 45 deg and their spatial frequency by more than two octaves. The general pattern of results obtained here, for the spatial domain, bares some similarities with masking results from the spatial-frequency domain. Tolhurst and Barfield (1978) used spatially extended sine-wave gratings while studying inter-frequency masking effects of spatially overlapping stimuli. They found threshold suppression when target and mask had similar frequencies and enhancement for frequencies differing by a factor of two or more. Our results show that the same phenomena exist in the space domain for localized signals. More than that, both effects seem to be of similar magnitude (0.4 log units) and in both cases the region of enhancement is wider and more pronounced. A comparison also can be made between the present results and those of Kulikowski and King-Smith (1973), who measured contrast threshold for a fine line in the presence of two flanking sub-threshold lines. Their results, which probably probe within filter integration processes (see Introduction), show enhancement for small mask to test distances (<0.05 deg) and suppression for larger distances up to 0.15 deg (compare with 2 deg, the maximal distance yielding enhancement in the present study). This reversed effect can be a result of using sub-threshold masks (Nachmias & Sansbury, 1974).

This pattern of results can be taken, as Tolhurst and Barfield (1978) already noted, as evidence for excitatory and inhibitory interactions in the space domain, in our case, and in the frequency domain, in their case. Based on their data they suggest: "Perhaps the channels are excited directly by frequencies up to about one octave from their optimum and are inhibited by a broader range of frequencies." Adopting their account for this phenomenon we suggest the existence of a similar pattern of connections in the space domain. That is,

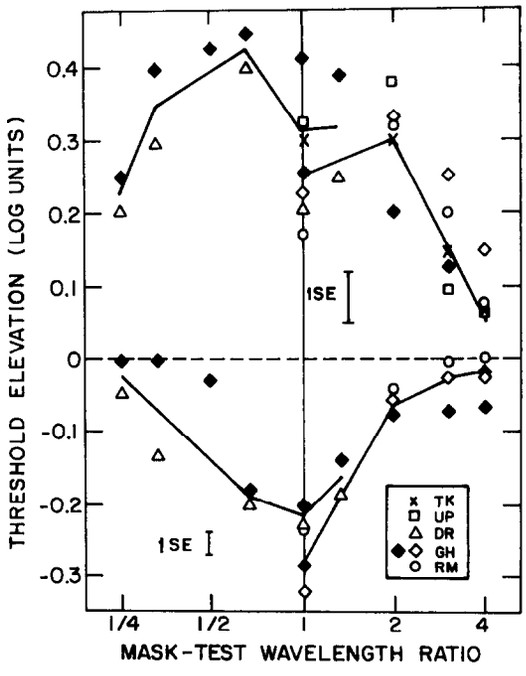

FIGURE 7. Maximal suppression and maximal enhancement as a function of mask–test wavelength ratio. The threshold elevation values were taken from curves as in Fig. 5, where maximal and minimal points were visually estimated. The curves were obtained by linear interpolation between observers' means. Observers RM, TK and UP were tested with $\lambda_t = 0.075$ deg, DR with $\theta_t = 0.225$ deg and GH with both λ_t.

channels are excited by other channels within a distance of two wavelengths from their location and are inhibited by channels from larger distances. These interactions do not have to be within the same layer of filters like in a network assuming feedback connection. An analogous outcome is expected from a feedforward scheme where higher level cells integrate the thresholded output of local band-limited filters, using an antagonistic weighting function. The parameters of this weighting function can be directly obtained from the present study: an excitatory center of two wavelengths radius surrounded by an inhibitory zone extending out up to a distance of eight wavelengths. These figures (2λ and 8λ) agree with the ones suggested previously (3λ and 9λ) for a similar mechanism involved in texture discrimination tasks (Sagi, 1990). While the inhibitory (enhancement) range seems to exceed the size of known spatial filters, e.g. 2λ (Watson, Barlow & Robson, 1983; Wilson, 1983), the excitatory (suppression) range largely overlaps with filter size and thus may reflect in part spatial integration within the filter receptive field. Within the context of this discussion it should be noted that the correspondence established here (and by Barfield and Tolhurst before us) between neuronal inhibition and sensitivity enhancement does not constitute a real paradox. Direct inhibition on the target area may reduce spontaneous activity (noise) at or near the area of detection and thus improve detection rate. On this account, the inhibition dependent enhancement is a threshold effect which should reverse once contrast judgment is made on an equivalent suprathreshold target. Evidence for such a suprathreshold phenomenon exists from contrast judgment studies (Chubb *et al.*, 1989; Sagi & Hochstein, 1985). Recently, Cannon and Fullenkamp (1991a) published detailed data describing the suppression of the apparent contrast of a small sine-wave grating patch by a high contrast surrounding grating. They find that the suppression effect can be described by a monotonic function, with suppression declining as the distance between target and surrounding grating increases. While the effect can be detected at distances up to ten wavelengths, it is most pronounced at a region extending to five wavelengths from the target center. In an additional study, Cannon and Fullenkamp (1991b) found some conditions under which contrast enhancement could be observed. Although only some of their observers showed this enhancement, the phenomenon seems to be consistent when stimulus contrast is low and surround width is small, implicating a contrast dependent mechanism.

Another possible account for the data presented here is a network assuming only inhibitory connections between neighboring filters. On this account, threshold suppression is a result of direct (strong) inhibition, while threshold enhancement is due to disinhibition. Thus, this model assumes some level of spontaneous activity which is sufficiently high to keep a steady inhibition between adjacent filters. Introducing a mask at some relatively large distance may cause inhibition upon channels neighboring the target, reducing their inhibiting output and thus improves target detection. This inhibitory model seems less plausible since the two regions we observed have different orientation (Fig. 5) and spatial-frequency (Fig. 7) tuning curves.

Regardless of the model adopted our data brings direct evidence for lateral spatial interactions between spatial filters. These interactions extend outside the range defined by linear integration within a single receptive field. It is encouraging that the spatial parameters obtained in this study for the different interaction ranges are consistent with previous experimental (Sagi, 1990) and theoretical (Rubenstein & Sagi, 1990) studies of human texture segmentation tasks. Long range interactions between cells of similar orientation were also observed recently in recordings from visual cortex (Gilbert & Wiesel, 1989; Grinvald, Ts'o, Frostig, Lieke, Arieli & Hildesheim, 1989) and it remains to be seen whether these interactions can serve as the underlying mechanism for the present psychophysical phenomena.

REFERENCES

Bouma, H. (1970). Interaction effects in parafoveal letter recognition. *Nature, 226*, 177–178.

Campbell, F. W. & Robson, J. G. (1968). Application of Fourier analysis to the visibility of gratings. *Journal of Physiology, London, 197*, 551–556.

Cannon, M. W. & Fullenkamp, S. C. (1991a). Spatial interactions in apparent contrast: Inhibitory effects among grating patterns different spatial frequencies, spatial positions and orientations. *Vision Research, 31*, 1985–1998.

Cannon, M. W. & Fullenkamp, S. C. (1991b). Lateral interactions among contrast sensitive mechanisms. *Journal of the Optical Society of America Annual, Technical Digest Series, 17*, 164.

Chubb, C., Sperling, G. & Solomon, J. (1989). Texture interactions determine apparent lightness. *Proceedings of the National Academy of Science U.S.A., 86*, 9631–9635.

Daugman, J. G. (1984). Spatial visual channels in the Fourier plane. *Vision Research, 24*, 891–910.

De Valois, K. K. (1977). Spatial frequency adaptation can enhance contrast sensitivity. *Vision Research, 17*, 1057–1065.

Flom, M. C., Heath, G. G. & Takahashi, E. (1963a). Contour interaction and visual resolution: Contralateral effects. *Science, 142*, 979–980.

Flom, M. C., Weymouth, F. W. & Khaneman, D. (1963b). Visual resolution and contour interaction. *Journal of the Optical Society of America, 53*, 1026–1032.

Gabor, D. (1946). Theory of communication. *Journal of the Institute of Electrical Engineers London, 93*, 429–457.

Gilbert, C. D. & Weisel, T. N. (1989). Columnar specificity of intrinsic horizontal and corticocortical connections in cat visual cortex. *Journal of Neuroscience, 9*, 2432–2442.

Graham, N. & Nachmias, J. (1971). Detection of grating patterns containing two spatial frequencies: A comparison of single channel and multichannel models. *Vision Research, 11*, 251–259.

Graham, N. & Robson, J. G. (1987). Summation of very close spatial frequencies: The importance of spatial probability summation. *Vision Research, 27*, 1997–2007.

Greenlee, M. W. & Magnussen, S. (1988). Interaction among spatial frequencies and orientation channels adapted concurrently. *Vision Research, 28*, 1303–1310.

Grinvald, A., Ts'o, D. Y., Frostig, R. D., Lieke, E., Arieli, A. & Hildesheim, R. (1989). Optical imaging of neuronal activity in the visual cortex. In Lam, D. M. K. & Gilbert, C. (Eds), *Neural mechanisms of visual perception* (pp. 117–135). Woodlands, Tex.: Portfolio.

Harvey, L. O. Jr & Doan, V. V. (1990). Visual masking at different polar angles in the two-dimensional Fourier plane. *Journal of the Optical Society of America, A, 7*, 116–127.

Kulikowski, J. J. & King-Smith, P. E. (1973). Spatial arrangement of line, edge and grating detectors revealed by subthreshold summation. *Vision Research, 13*, 1455–1478.

Kulikowski, J. J., Abadi, R. & King-Smith, P. E. (1973). Orientation selectivity of grating and line detectors in human vision. *Vision Research, 13*, 1479–1486.

Nachmias, J. & Sansbury, R. V. (1974). Grating contrast: Discrimination may be better than detection. *Vision Research, 14*, 1039–1042.

Rubenstein, B. S. & Sagi, D. (1990). Spatial variability as a limiting factor in texture discrimination tasks: Implications for performance asymmetries. *Journal of the Optical Society of America, A, 7*, 1632–1643.

Sachs, M. B., Nachmias, J. & Robson, J. G. (1971). Spatial-frequency channels in human vision. *Journal of the Optical Society of America, 61*, 1176–1186.

Sagi, D. (1990). Detection of an orientation singularity in gabor textures: Effect of signal density and spatial-frequency. *Vision Research, 30*, 1377–1388.

Sagi, D. & Hochstein, S. (1983). Discriminability of suprathreshold compound spatial frequency gratings. *Vision Research, 23*, 1595–1606.

Sagi, D. & Hochstein, S. (1985). Lateral inhibition between spatially adjacent spatial-frequency channels? *Perception and Psychophysics, 37*, 315–322.

Sagi, D. & Polat, U. (1992). Perceptual learning increase the range of inhibitory connections between spatial filters. *Perception (Suppl. 2), 21*, 69.

Tolhurst, D. J. & Barfield, L. P. (1978). Interaction between spatial-frequency channels. *Vision Research, 18*, 951–958.

Watson, A. B. (1982). Summation of gratings patches indicates many types of detectors at one retinal location. *Vision Research, 22*, 17–25.

Watson, A. B., Barlow, H. B. & Robson, J. G. (1983). What does the eye see best? *Nature, 302*, 419–422.

Westheimer, G. (1967). Spatial interaction in human cone vision. *Journal of Physiology, London, 190*, 139–154.

Wilson, H. R. (1983). Psychophysical evidence for spatial channels. In Braddick, O. J. & Sleigh, A. C. (Eds), *Physical and biological processing of images*. Berlin: Springer.

Wilson, H. R., McFarlane, D. K. & Phillips, G. C. (1983). Spatial frequency tuning of orientation selective units estimated by oblique masking. *Vision Research, 23*, 873–882.

Acknowledgements—We would like to thank Alexander Cooperman, Avi Karni and Barton Rubenstein for helpful discussions and comments on the manuscript, Leah Mory Rauch and Nava Shaya for helping with the software used in the experiments and Yehuda Barbut for the graphics. This work was supported by the Basic Research Foundation administered by the Israel Academy of Sciences and Humanities.